© 2017. Published by The Company of Biologists Ltd | Journal of Cell Science (2017) 130, 1333-1340 doi:10.1242/jcs.198408

TOOLS AND TECHNIQUES

Localization of phosphorylated connexin 43 using serial section immunogold electron microscopy

Rachael P. Norris*, Valentina Baena and Mark Terasaki*

ABSTRACT

Gap junction turnover occurs through the internalization of both of the plasma membranes of a gap junction plaque, forming a double membrane-enclosed vesicle, or connexosome. Phosphorylation has a key role in regulation, but further progress requires the ability to clearly distinguish gap junctions and connexosomes, and to precisely identify proteins associated with them. We examined, by using electron microscopy, serial sections of mouse preovulatory ovarian follicles that had been collected with an automated tape collecting ultramicrotome (ATUM). We found that connexosomes can form from adjacent cell bodies, from thin cell processes or from the same cell. By immunolabeling serial sections, we found that residue S368 of connexin 43 (also known as GJA1) is phosphorylated on gap junctions and connexosomes, whereas connexin 43 residue S262 is phosphorylated only on some connexosomes. These data suggest that phosphorylation at S262 contributes to connexosome formation or processing, and they provide more precise evidence that phosphorylation has a key role in gap junction internalization. Serial section electron microscopy of immunogold-labeled tissues offers a new way to investigate the three-dimensional organization of cells in their native environment.

KEY WORDS: Connexin, Annular gap junctions, Immunogold, Serial section electron microscopy, Connexosomes, Phosphorylation

INTRODUCTION

Gap junctions are an important means for cell–cell communication. They allow for the direct passage of molecules 1 kDa or less in size through pore-containing complexes (connexons), which are docked head-to-head between two cells. Connexons are hexamers of the transmembrane protein family of connexins (Kumar and Gilula, 1992; Goodenough et al., 1996). Mutations in many of the 21 different connexin genes cause human pathologies, underscoring their importance in development (White and Paul, 1999; Dobrowolski and Willecke, 2009).

Gap junction turnover begins with the internalization of a large part, or possibly the entire gap junction, into one of the two cells and is followed by degradation in the lysosome (Watanabe et al., 1988; Jordan et al., 2001; Piehl et al., 2007). The internalization event results in a remarkable structure, the connexosome (Laird, 2006), which is a double membrane-enclosed vesicle that possesses within it the plasma membrane and cytoplasm of another cell. This is also sometimes referred to as an annular gap junction.

Department of Cell Biology, University of Connecticut Health Center, Farmington, CT 06030, USA.

*Authors for correspondence (Norris@uchc.edu; terasaki@uchc.edu)

R.P.N., 0000-0003-1711-965X; M.T., 0000-0003-4964-9401

Received 7 October 2016; Accepted 9 February 2017

Connexin 43 (Cx43; also known as GJA1), the most widely expressed connexin, is phosphorylated *in vivo* on at least 12 serine and 2 tyrosine residues by several different kinases (Solan and Lampe, 2016). There is much evidence that Cx43 phosphorylation regulates gap junction turnover. The development of phosphorylation-specific antibodies made it possible to monitor the phosphorylation status of many of these sites by western blotting (Lampe et al., 2006). Patterns and sequences of phosphorylation changes have been observed in wounded skin, ischemic hearts and cultured cells stimulated with growth factors (Smyth et al., 2014; Falk et al., 2016; Solan and Lampe, 2016). In western blots, entire cells are solubilized and probed with an antibody. Changes in phosphorylation levels are compared with the relative amounts of gap junctions and connexosomes as assessed from imaging data from pan-connexin immunofluorescence or thin-section transmission electron microscopy. This does not directly determine whether gap junctions or connexosomes are differentially phosphorylated. There are some antibodies to phosphorylated epitopes that are effective for immunolocalization, which can be imaged directly; however, there are additional difficulties. Gap junctions and connexosomes have a wide range of dimensions, ∼0.3–3 µm (Espey and Stutts, 1972; Larsen, 1977), so some of them are near to the lateral and *z* resolution of light microscopy, making it sometimes difficult to distinguish them. Electron microscopy methods have greater resolution but usually produce an image of a single section through a complex three-dimensional organization, so that an apparent connexosome could be a cross section through an indented gap junction. Improvements in the imaging of gap junctions and connexosomes therefore would help in understanding the role of phosphorylation in gap junction turnover.

Recently, a large improvement in serial section electron microscopy has been made through the development of the automated tape collecting ultramicrotome (ATUM), which is coupled with imaging by scanning electron microscopy (Kasthuri et al., 2015). We used this approach to characterize gap junctions and connexosomes in mouse ovarian follicles and extended the technique to post-embedding immunogold labeling to localize phosphorylated forms of Cx43.

RESULTS

Characterization of connexosomes

Ring-shaped gap junctions are seen in single thin-section transmission electron micrographs from various tissues, including ovarian granulosa cells (Fig. 1A). Serial sections are required to distinguish whether these are a cross section through a connexosome or an invaginated gap junction (Fig. 1B) (Espey and Stutts, 1972; Merk et al., 1973).

We used a field-emission scanning electron microscope for imaging serial sections, which has a lower resolution than transmission electron microscopy. Although the two membrane bilayers making up a ring-shaped gap junction could not be resolved, we were able to distinguish them by their darker thicker

Journal of Cell Science (2017) 130, 1333-1340 doi:10.1242/jcs.198408

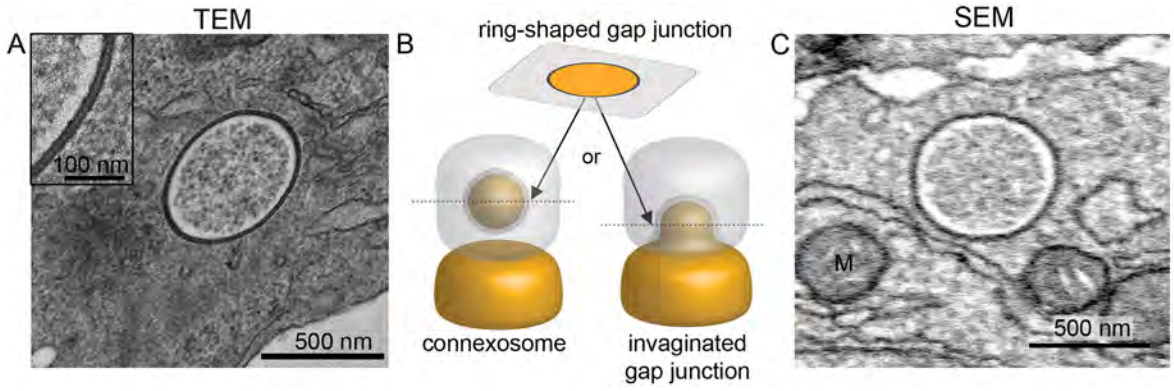

Fig. 1. Ring-shaped gap junctions using transmission electron microscopy or scanning electron microscopy. (A) A ring-shaped gap junction profile in an ovarian granulosa cell imaged by transmission electron microscopy (TEM). Inset shows a higher magnification view of the double membranes. Note the electron-lucid area next to the inner membrane. (B) A schematic illustration showing that a ring-shaped gap junction, as seen in A, could be a cross section through a fully internalized gap junction (connexosome) or an invaginated gap junction. (C) A ring-shaped gap junction in an ovarian granulosa cell imaged by scanning electron microscopy (SEM). These were identified in micrographs by their characteristic thick electron-dense membrane and the lucid area just inside the membrane. M, mitochondrion.

membrane, the lucid area just inside the membrane, their round shape and their diameter of 200–800 nm (Fig. 1C) (Espey and Stutts, 1972; Merk et al., 1973; Falk, et al., 2016). While smaller connexosomes are in the size range of secretory vesicles, they are still distinguishable by their characteristic electron-density pattern.

To quantify the proportion of ring-shaped structures that represented connexosomes, we analyzed two 50×50×20 µm volumes (500 sections of 40 nm thickness). This volume includes approximately 130–190 individual cells of 8–9 µm in diameter. Our analysis showed that 92% of ring-shaped gap junctions (158 out of 171) were connexosomes. A representative connexosome, identified by a series of sections, is shown in Fig. 2A. The other 8% (13 of 171) were invaginated gap junctions, presumably in the process of becoming connexosomes. In several cases, this was an invaginated gap junction between two adjoining cell bodies (4 of 13). Unexpectedly, in six cases, the invaginated gap junction was forming from the end of a thin cell process (2–5 µm long) (Fig. 2B,D; Movies 1 and 2) and, in three cases, it was forming from a process originating from the same cell, termed a ‘reflexive gap junction’ (Herr, 1976) (Fig. 2C,D). These observations show that most ring-shaped gap junctions are connexosomes and that these can originate from an adjacent cell body, a cell process or from the same cell (Fig. 2D).

Cx43 immunolocalization on serial sections

Gap junctions between ovarian granulosa cells are primarily comprised of Cx43 (Okuma et al., 1996). Therefore, to advance our capability to investigate a link between Cx43 phosphorylation and gap junction turnover, we adapted methods for post-embedding immunolabeling (Rubio and Wenthold, 1997) to work in conjunction with the ATUM method. Serial sections of lowicryl-HM20-embedded tissue on tape were probed with an antibody against Cx43, followed by a secondary antibody conjugated to gold particles. Both gap junctions and internalized gap junctions were clearly distinguishable and labeled for Cx43 (Fig. 3A; Movie 3). Although tissue morphology is compromised when samples are prepared for immunogold labeling (Mühlfeld and Richter, 2006), it was possible in most cases to determine whether a ring-shaped gap junction was a connexosome (Fig. 3B) or whether it was an invaginated gap junction (Fig. 3C). Since we had already found that 92% of ring-shaped gap junctions in this tissue are connexosomes, for convenience we will refer to them as connexosomes. In a volume of 60×60×7 µm, we found that 100% of connexosomes (n=37) were positive for total Cx43.

Cx43 phosphorylation on residues S368 and S262 in connexosomes and gap junctions

To test whether particular phosphorylated forms of Cx43 are differentially distributed between connexosomes and gap junctions, we focused on residues S368 and S262. These are protein kinase C (PKC) and MAP kinase phosphorylation sites that are associated with gap junction internalization, and for which well-characterized antibodies are available (Nimlamool et al., 2015; Solan and Lampe, 2016). We found that essentially all connexosomes and gap junctions were phosphorylated on Cx43 residue S368 (Fig. 4A,B; Movie 4). From five fields of view encompassing a 60×60×7 µm volume, 33 out of 34 connexosomes and 21 out of 21 gap junctions could be identified as containing Cx43 phosphorylated at S368 (Fig. 5D).

In contrast, an antibody to phosphorylated S262 of Cx43 labeled approximately half of the connexosomes (23 out of 48, or 48%) and 0 out of 18 gap junctions in six fields of view totaling a 60×60×7 µm volume (Fig. 5). To confirm that connexosomes and gap junctions that were negative for Cx43 phosphorylated at S262 were positive for total Cx43, we performed double labeling. Since individual gap junctions and connexosomes span several sections, it is possible to immunolocalize two (or more) epitopes by labeling adjacent sections with different antibodies (Fig. 6). This allows one to use antibodies from the same source (e.g. rabbit) and the same size gold particles, whereas double labeling on single sections requires careful titration of two antibodies from different sources (e.g. rabbit and mouse) and secondary antibodies with different size gold particles. When we examined adjacent groups of sections labeled with antibodies to either total Cx43 or that phosphorylated at S262, we confirmed that some connexosomes labeled with total Cx43 were also positive for phosphorylation at S262 (Fig. 7A, top row; Movie 5) while others were not (Fig. 7A, bottom row). Gap junctions that were positive for total Cx43 were not positive for phosphorylation at S262 (Fig. 7B).

These results indicate that many, but not all, connexosomes have Cx43 phosphorylated on S262. A deeply invaginated gap junction connected by a thin cell process (Fig. 2B) is difficult to discern in Lowicryl sections due to the compromised morphology. However, these comprise less than 4% (6 out of 171) of all ring-shaped gap

Journal of Cell Science (2017) 130, 1333-1340 doi:10.1242/jcs.198408

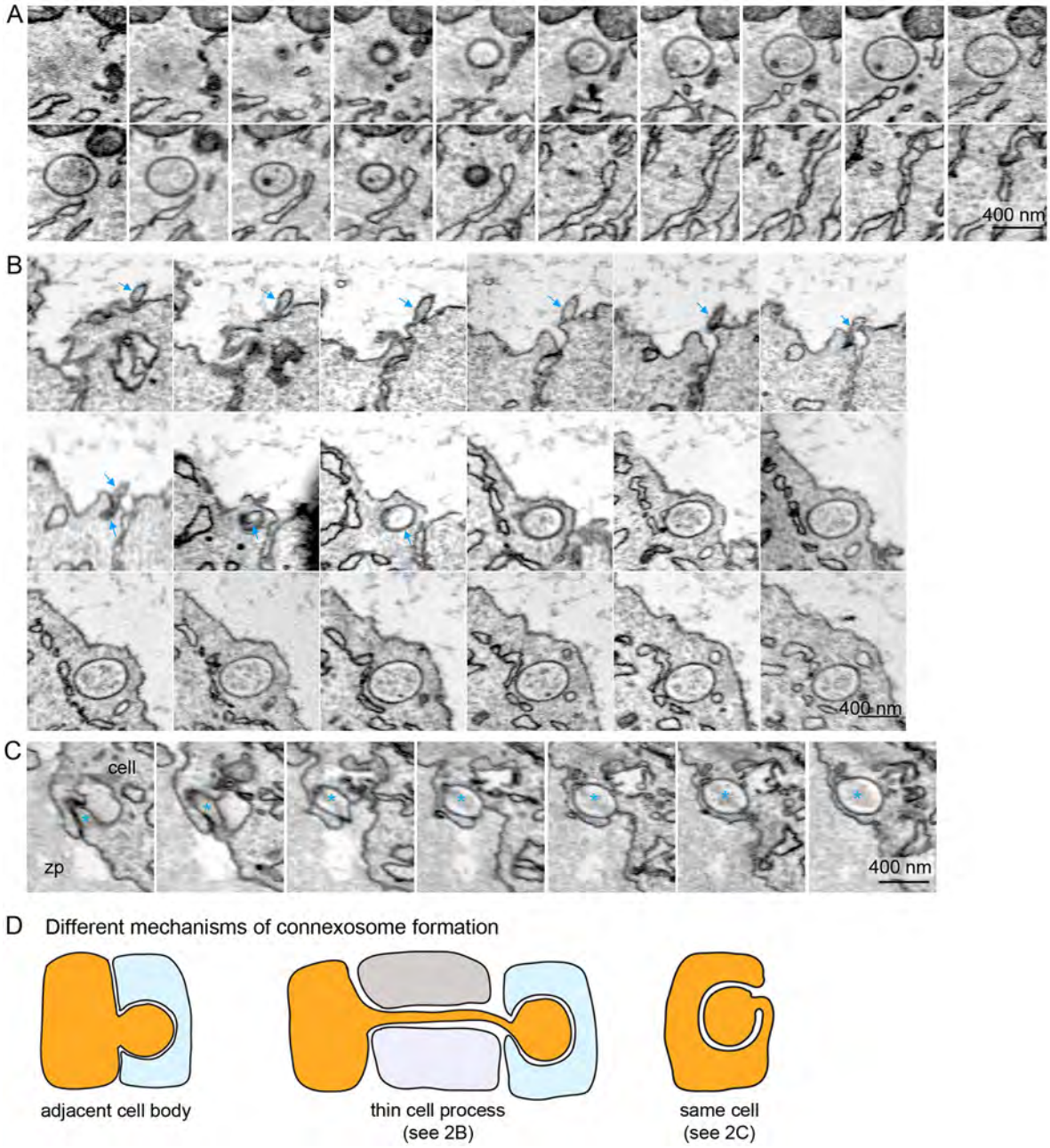

Fig. 2. Characterization of connexosomes. (A) Serial sections (40 nm thickness) of a fully internalized gap junction (connexosome) viewed by scanning electron microscopy. (B) Serial sections through a structure that appears to be a forming connexosome between a granulosa cell process (blue arrow) interacting with another granulosa cell. (C) Serial sections showing a cell process (blue asterisk) that interacts with another part of the same cell to form a ring-shaped gap junction. Gap junctions between different parts of the same cell are called 'reflexive gap junctions'. This structure was found in an ovarian granulosa cell next to the specialized extracellular matrix from the oocyte called the zona pellucida (zp). (D) Summary of different mechanisms by which connexosomes may form, found by examining serial sections. Connexosomes may originate from an adjacent cell body, from a thin cell process (as in B) or from a process from the same cell (as in C).

junctions in epon-embedded sections, so these structures may be phosphorylated on S262 but they do not encompass the entire sub-population of connexosomes that have Cx43 phosphorylated at residue S262.

DISCUSSION

The ATUM method is one of several new methods that has been developed for the comprehensive documentation of synaptic connections (Denk and Horstmann, 2004; Kasthuri et al., 2015; Micheva and Smith, 2007; Collman et al., 2015). Here, we show that this method is well suited to studying the mechanisms involved in gap junction internalization and turnover. With the improved ability to discern the three-dimensional structures of ring-shaped gap junctions, we found that most of these structures in ovarian granulosa cells are connexosomes. Invaginating gap junctions seem likely to be intermediates in the formation of connexosomes. Surprisingly, some invaginating gap junctions were present at the ends of thin cell processes, and some were formed between a cell process and a different area of the same cell. While gap junctions have been found at the ends of cell processes in granulosa cells (Merk et al., 1973) and chick limb buds (Kelley and Fallon, 1978), and reflexive gap junctions have been found in ovaries (Herr, 1976),

Journal of Cell Science (2017) 130, 1333-1340 doi:10.1242/jcs.198408

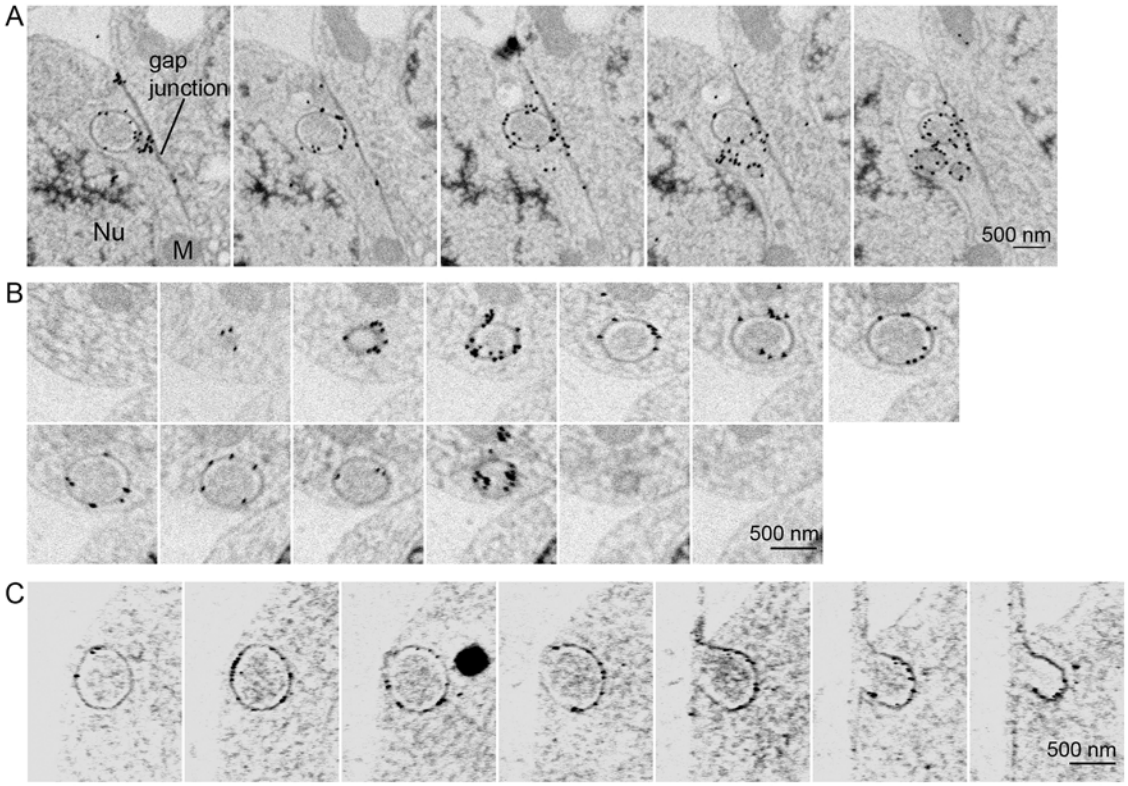

Fig. 3. Immunolocalization of total Cx43 in serial sections. (A) Serial sections of gap junctions labeled for total Cx43 using a 15 nm gold-conjugated secondary antibody. In this cell, a gap junction is directly adjacent to a group of connexosomes. (B) Serial sections of a connexosome labeled for total Cx43 using a 15 nm gold-conjugated secondary antibody. (C) Serial sections of an invaginated gap junction labeled for total Cx43 and 15 nm gold-conjugated secondary antibody. All tissue sections in A–C were 60 nm thick. M, mitochondrion; Nu, nucleus.

our findings provide the first evidence that connexosomes can form from these types of cell interactions.

Our findings show that immunolocalization of phosphorylated Cx43 sites is best done with serial sections in order to identify which intermediate in gap junction internalization is labeled. Serial section microscopy has traditionally been performed by cutting ribbons, collecting them on unsupported formvar and viewing them using transmission electron microscopy. To immunolabel this fragile preparation is technically very challenging and has very rarely been done. To use immunogold labeling with the other new approaches to serial sectioning – i.e. serial block face and focused ion beam scanning electron microscopy (FIB-SEM) – would require removing the block from the vacuum and applying antibodies between every cut. On the other hand, it is very feasible to immunolabel sections collected on tape. By extending the ATUM method to work with immunogold-labeled tissues, we can now

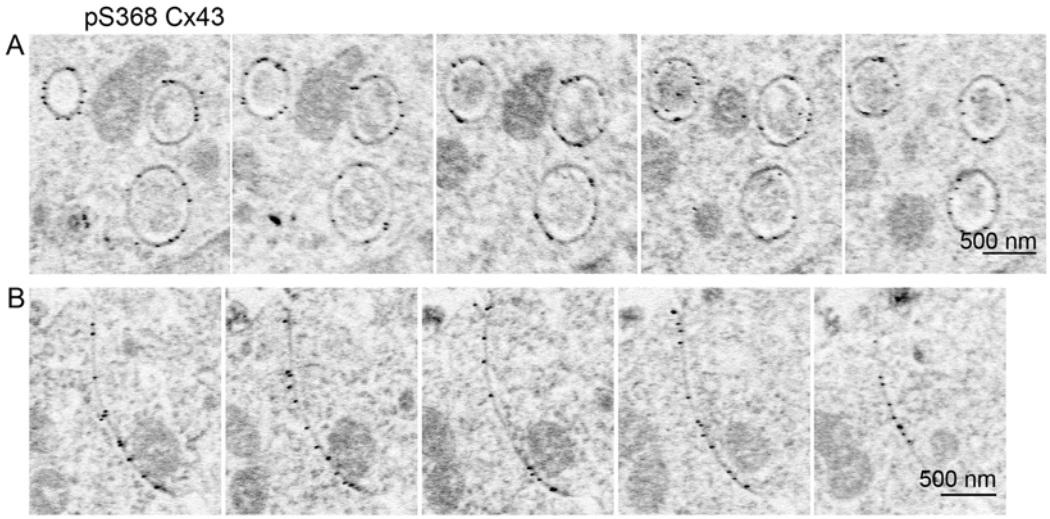

Fig. 4. Cx43 is phosphorylated on S368 in connexosomes and gap junctions. (A) Serial sections of connexosomes labeled for Cx43 phosphorylated at S368 (pS368 Cx43) and 10 nm gold-conjugated secondary antibody. Smaller gold particles were used to increase the available signal of antibodies detecting phosphorylated Cx43. (B) Serial sections of a gap junction labeled for Cx43 phosphorylated at S368. All tissue sections in A and B were 60 nm thick.

Journal of Cell Science (2017) 130, 1333-1340 doi:10.1242/jcs.198408

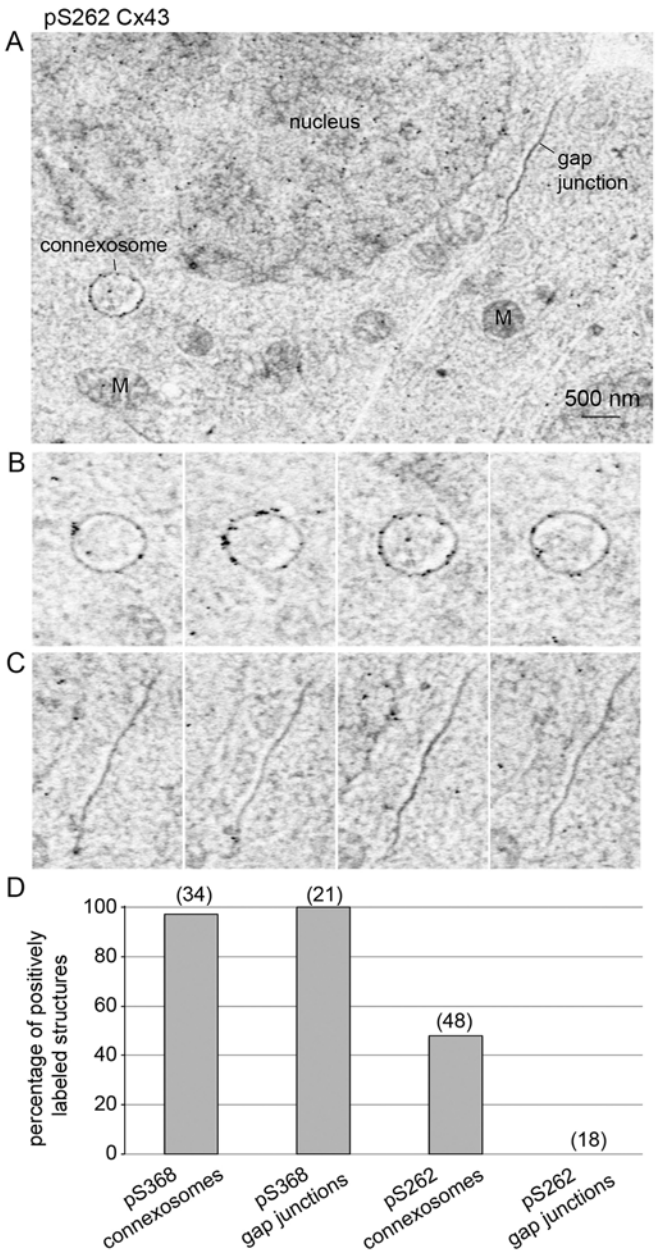

Fig. 5. Cx43 is phosphorylated on S262 only in connexosomes. (A) Overview of a section stained for Cx43 phosphorylated at S262 (pS262 Cx43) and 10 nm gold-conjugated secondary antibody, in which a connexosome is labeled but a gap junction is not. (B) Serial sections of the connexosome shown in A that was positive for pS262 Cx43. (C) Serial sections of the gap junction shown in A that were not positive for pS262 Cx43. All tissue sections in A–C were 60 nm thick. (D) Quantification of gap junctions and connexosomes labeled with phosphorylated-Cx43-specific antibodies. The sample number is in parentheses above each column.

distinguish Cx43 that is localized to gap junctions at the plasma membrane from invaginated gap junctions or from connexosomes in close proximity to the plasma membrane. It would not be possible to resolve these structures using light microscopy.

When assayed by western blotting, phosphorylation of both residues S262 and S368 occurs in parallel with decreased gap junction permeability in TPA-treated cells (Sirnes et al., 2009) and with increased gap junction turnover in VEGF-stimulated porcine aortic endothelial cells (Nimlamool et al., 2015). The use of kinase inhibitors suggests that phosphorylation on the PKC site S368 is upstream of phosphorylation on the MAP kinase site S262 (Sirnes et al., 2009; Nimlamool et al., 2015).

We investigated Cx43 phosphorylation in mouse ovarian follicles at a stage at which they await stimulation by luteinizing hormone in order to undergo ovulation. We found that phosphorylation of Cx43 on residue S368 occurred in both gap junctions and connexosomes. This observation is not inconsistent with the western blot studies referenced above since it is possible that increased phosphorylation at S368 occurs on one or both of these structures when gap junction turnover is stimulated.

We also found that phosphorylation of Cx43 on S262 was localized to approximately half of connexosomes. The significance of S262 phosphorylation in a subset of connexosomes remains to be determined. Connexosomes may be phosphorylated temporally, for instance, just before their formation and then get dephosphorylated when targeted for destruction. Alternatively, a sub-population of connexosomes may be marked for a different fate or function depending on their location in the cell or interaction with a specific organelle.

The means now exist to strengthen or refine current models of gap junction turnover in terms of the sequence and location of Cx43 phosphorylation and interaction with other proteins. Specifically, we can now study the regulation of gap junction internalization in ovarian follicles at various stages of development in greater depth. During meiotic resumption, gap junction internalization increases dramatically (Larsen et al., 1987), and phosphorylation of S262 and of other MAP kinase sites increases transiently (Norris et al., 2008). With the ability to double label structures by using adjacent sections, we can explore whether phosphorylation on particular sites occurs in the same connexosomes, and whether these connexosomes associate exclusively with other proteins or cell components.

By adapting the ATUM method of collecting and imaging serial sections of tissue to work with post-embedding immunogold labeling of proteins, cellular structures are easily identified, and labeling of consecutive sections increases the antibody signal and serves to evaluate reproducibility. We also show that double- or multi-labeling is very feasible if a structure of interest spans several sections, meaning that sections can be labeled individually with different antibodies. The new serial sectioning methods for electron microscopy, originally developed for determining synaptic connectivity, now combined with the ability to immunolocalize proteins, provide new ways to investigate the three-dimensional organization of cells in their native environment.

MATERIALS AND METHODS

Mice

25- to 27-day-old C57Bl/6J female mice (*Mus musculus*) from The Jackson Laboratories (Bar Harbor, ME) were used in all experiments. All studies with mice were in accordance with guidelines published by the National Institutes of Health and approved by the UConn Health Institutional Animal Care and Use Committee. Mice were housed in a temperature- and humidity-controlled environment with water and food available *ad libitum*.

Preparation of ovarian follicles for electron microscopy

Ovaries from an equine chorionic gonadotropin (eCG)-primed 25-day-old mouse were manually isolated and cut into smaller pieces for fixation in 2.5% glutaraldehyde, 2% paraformaldehyde and 0.1 M cacodylate buffer for 3.5 h (all chemicals from Electron Microscopy Sciences, Hatfield, PA). Samples were rinsed with cold 0.1 M cacodylate buffer, then post-fixed in fresh 2% osmium tetroxide and 1.5% potassium ferrocyanide for 1 h at room temperature. Samples were rinsed in water and then left in 1% aqueous uranyl acetate overnight at 4°C. The following day, tissues were rinsed in water and then incubated in lead aspartate for 30 min at 60°C (Walton,

Journal of Cell Science (2017) 130, 1333-1340 doi:10.1242/jcs.198408

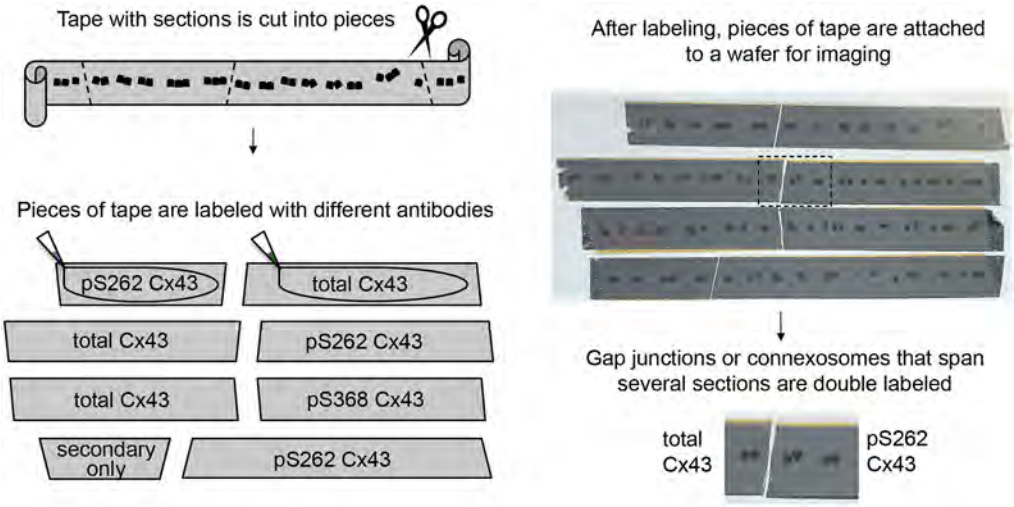

Fig. 6. Double labeling of gap junctions or connexosomes. Schematic drawing demonstrating the protocol used for double labeling of structures that span several sections. First, the tape is cut into pieces. Next, different antibodies are applied to adjacent sections on separate pieces of tape. Pieces of tape are then attached to a wafer for imaging, and any structures that span two pieces of tape are double labeled. pS262 Cx43, antibody against Cx43 phosphorylated at S262; pS368 Cx43, antibody against Cx43 phosphorylated at S368.

1979). After rinsing in water, tissue was dehydrated in graded ethanol concentrations for at least 10 min per solution. Samples were then washed with propylene oxide and infiltrated with increasing concentrations of Poly/Bed resin (Polysciences, Warrington, PA) and polymerized at 60°C for 1–2 days.

Preparation of follicles for post-embedding immunogold labeling

Ovarian follicles, 360–400 µm in diameter, were manually isolated from an eCG-primed 27-day-old mouse. The follicles were cultured on Millicell membranes in 10 ng/ml follicle-stimulating hormone (FSH) for 24–25 h, as described previously by Norris et al., 2008, with the substitution of 3 mg/ml bovine serum albumin (BSA) for serum. Follicles were then transferred to brass specimen carriers and high-pressure frozen with an EMPACT 2 instrument (Leica, Buffalo Grove, IL). From this point, we followed the procedure of Rubio and Wenthold (1997). Samples were freeze-substituted with 1.5% uranyl acetate in dry methanol for 43 h at −90°C, rinsed in methanol, and infiltrated with Lowicryl HM-20 (Electron Microscopy Sciences, Hatfield, PA) and then polymerized with ultraviolet light in an AFS 2 freeze substitution unit (Leica).

Collection of serial sections

Ultrathin sections of Poly/Bed- (40 nm) or Lowicryl- (60 nm) embedded tissues were cut on a UC-7 ultramicrotome (Leica) with a diamond knife (Diatome, Hatfield, PA). The sections were picked up by an automated tape collector on glow-discharged kapton tape (Kasthuri et al., 2015; Terasaki et al., 2013).

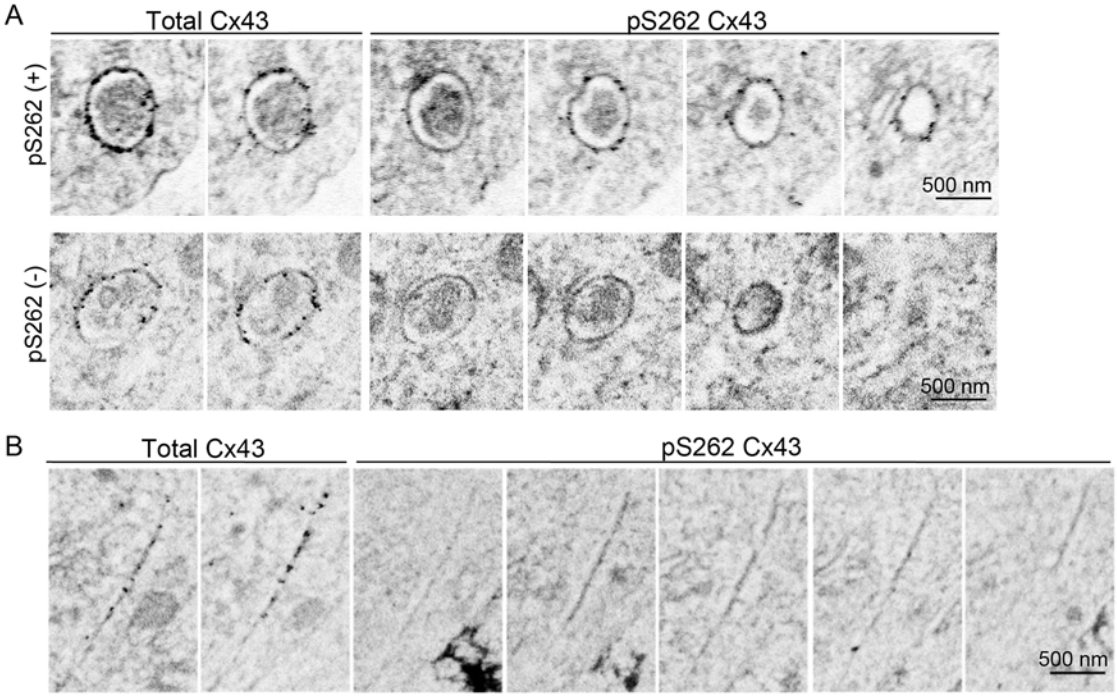

Fig. 7. Double labeling for total Cx43 and Cx43 phosphorylated at S262. (A) Serial sections of connexosomes labeled for total Cx43 or for Cx43 phosphorylated at S262 (pS262 Cx43) in adjacent groups of sections, followed by staining with 10 nm gold-conjugated secondary antibody. Top row: a connexosome labeled for total Cx43 and that is also positive for staining of pS262 Cx43 [pS262 (+)]. Bottom row: a connexosome that is also labeled for total Cx43 but that is not positive for pS262 Cx43 [pS262 (–)]. (B) Serial sections of a representative gap junction labeled for total Cx43 or for pS262 Cx43 in adjacent sections, followed by staining with 10 nm gold-conjugated secondary antibody. Gap junctions were positive for total Cx43 but were not phosphorylated on S262 of Cx43. All tissue sections in A and B were 60 nm thick.

Journal of Cell Science (2017) 130, 1333-1340 doi:10.1242/jcs.198408

Immunogold staining of serial sections

Ribbons of tissue sections on kapton tape were cut to lengths of 1–3 inches and then adhered to parafilm for immunostaining. For double labeling of connexosomes or gap junctions, adjacent groups of sections on separate pieces of tape were incubated with different primary antibodies in separate staining dishes to avoid any mixing of antibodies. Sections were rehydrated with 1× PBS (Life Technologies, Grand Island, NY) and blocked in 5% normal goat serum (Invitrogen, Frederick, MD) in a solution of 1% BSA in PBS. Sodium fluoride (10 mM final) was added to buffers used with phosphorylation-specific antibodies to inhibit phosphatase activity. Primary antibodies and dilutions used were as follows: anti-Cx43 produced in rabbit (#C6219, Sigma-Aldrich, St. Louis, MO) used at 1:50 for a final concentration of ∼15 µg/ml; anti-phosphorylated-Cx43 (S368) (#3511, Cell Signaling Technology, Danvers, MA) used at 1:10, for a final concentration of ∼3 µg/ml; and anti-phosphorylated-Cx43 (S262) (#sc-17219-R, Santa Cruz Biotechnology, Dallas, TX) used at 1:2, for a final concentration of ∼100 µg/ml. All antibodies were affinity purified.

Following a 2 h incubation at room temperature or an overnight incubation at 4°C with primary antibody, sections were rinsed three times for 5 min each in PBS, then rinsed once in 1% BSA in PBS. Next, 10 or 15 nm gold particle-conjugated goat anti-rabbit IgG antibody (#25108 and #25112, Electron Microscopy Sciences) was diluted 1:20 and applied to sections for 1 h at room temperature. Sections were then rinsed with 1× PBS followed by Milli-Q filtered water and dried overnight. If sections were stained with different antibodies in separate dishes, they were placed back in their original order and post-stained with 5–6% uranyl acetate in 50% methanol with water for 10–15 min, then rinsed generously in water.

Imaging serial sections of tissue with scanning electron microscopy

Immunolabeled Lowicryl- or Poly/Bed-embedded tissue sections on tape were attached to a 10-cm-diameter silicon wafer (University Wafer, South Boston, MA) with double-sided carbon adhesive tape (Electron Microscopy Sciences). Wafers were carbon coated (Denton, Moorestown, NJ) and imaged on a Sigma field-emission scanning electron microscope (Zeiss, Thornwood, NY) using a backscatter detector. Sections were imaged with 8 keV electrons, 120 µm aperture, a detector at high gain and 1–2 µs dwell time. Atlas software (version 4.0, Fibics, Ottawa, Canada) was used for automatic imaging of serial sections. The Atlas software was used to set the resolution, pixel width, auto-focus and other settings required for automatic acquisition. The initial map, which was generated from a photograph, was used to obtain low-resolution images of entire preovulatory follicles. These images were aligned with the FIJI macro Register Virtual Stack Slices (http://imagej.net), which yields information to make a more accurate map of the section rotation and location. This second map was used to take higher resolution images of various regions of granulosa cells within the follicle, which were used to make a map accurate to within a few microns, which is the accuracy of the motorized stage. The mapping procedures were performed using a combination of ImageJ/FIJI macros and custom python (http://python.org) scripts to modify the XML files that the Atlas software uses to locate each section. The final high-resolution images of various regions within follicles, including cumulus cells and mural granulosa cells, were taken at 4–6 nm/pixel resolution, with a field of view of 50–75 mm^2. We found that scanning the tissues that had been embedded in Lowicryl at low magnification before zooming in to look in more detail was beneficial. Some sections in Lowicryl were prone to damage during imaging.

Analyzing images for connexosome shape and immunolocalization

After images were obtained, lower resolution images were aligned using the Register Virtual Stack Slices macro (FIJI), then larger files were aligned and diced for convenient viewing with a custom program (Piet, provided by Duncan Mak and Jeff Lichtman, Harvard University, Cambridge, MA). These files were used to track and analyze individual gap junctions to determine the three-dimensional shape and to analyze immunogold labeling. Our criteria for positive immunogold labeling of connexosomes was that at least half of the sections through a connexosome had one or more gold particles and that all sections combined had at least five gold particles in total. Our criteria for positive immunogold labeling of gap junctions was that flat or slightly curved junctions between two cells labeled for total Cx43 had a total of at least 14 gold particles within three or more sections. Gap junctions considered positive for phosphorylated Cx43 had a total of at least 11 gold particles within three or more serial sections adjacent to gap junctions positive for total Cx43. The mean total was 32 particles per gap junction.

Measuring cell processes

Image stacks were imported into the TrakEM2 program in FIJI to measure the lengths of cell processes involved in connexosome formation. ‘Treelines’ were created to record the distances of cell processes through the sections from the point at which they could be first viewed until they became a rounded gap junction. In three cases, a cell process continued beyond the sections that were available for imaging, therefore the cell process length was recorded as a minimal length.

Acknowledgements

We thank Jeff Lichtman for the idea of double-labeling serial sections; Tom Reese for useful discussions; Maria Rubio for advice on immunolabeling; Art Hand and Maya Yankova for advice and support with processing samples; and Rindy Jaffe, Maria Rubio, Art Hand, Maya Yankova and Paul Lampe for critical review of the manuscript.

Competing interests

The authors declare no competing or financial interests.

Author contributions

Conceptualization and Methodology: R.P.N., V.B. and M.T. Investigation: R.P.N., V.B. and M.T. Writing - original draft preparation: R.P.N. and M.T. Writing - review and editing: R.P.N., V.B. and M.T. Resources, Supervision and Funding acquisition: M.T.

Funding

This work was supported by a grant to R.P.N. from the Fund for Science, and a grant to M.T. from the Connecticut Science Fund.

Supplementary information

Supplementary information available online at
http://jcs.biologists.org/lookup/doi/10.1242/jcs.198408.supplemental

References

Collman, F., Buchanan, J., Phend, K. D., Micheva, K. D., Weinberg, R. J. and Smith, S. J. (2015). Mapping synapses by conjugate light-electron array tomography. *J. Neurosci.* **35**, 5792-5807.

Denk, W. and Horstmann, H. (2004). Serial block-face scanning electron microscopy to reconstruct three-dimensional tissue nanostructure. *PLoS. Biol.* **2**, e329.

Dobrowolski, R. and Willecke, K. (2009). Connexin-caused genetic diseases and corresponding mouse models. *Antioxid. Redox. Signal.* **11**, 283-295.

Espey, L. L. and Stutts, R. H. (1972). Exchange of cytoplasm between cells of the membrana granulosa in rabbit ovarian follicles. *Biol. Reprod.* **6**, 168-175.

Falk, M. M., Bell, C. L., Kells Andrews, R. M. and Murray, S. A. (2016). Molecular mechanisms regulating formation, trafficking and processing of annular gap junctions. *BMC Cell Biol.* **17** Suppl. 1, S22.

Goodenough, D. A., Goliger, J. A. and Paul, D. L. (1996). Connexins, connexons, and intercellular communication. *Annu. Rev. Biochem.* **65**, 475-502.

Herr, J. C. (1976). Reflexive gap junctions: gap junctions between processing arising from the same ovarian decidual cell. *J. Cell Biol.* **69**, 495-501.

Jordan, K., Chodock, R., Hand, A. R. and Laird, D. W. (2001). The origin of annular junctions: a mechanism of gap junction internalization. *J. Cell Sci.* **114**, 763-773.

Kasthuri, N., Hayworth, K. J., Berger, D. R., Schalek, R. L., Conchello, J. A., Knowles-Barley, S., Lee, D., Vázquez-Reina, A., Kaynig, V., Jones, T. R. et al. (2015). Saturated reconstruction of a volume of Neocortex. *Cell* **162**, 648-661.

Kelley, R. O. and Fallon, J. F. (1978). Identification and distribution of gap junctions in the mesoderm of the developing chick limb bud. *J. Embryol. Exp. Morphol.* **46**, 99-110.

Kumar, N. M. and Gilula, N. B. (1992). Molecular biology and genetics of gap junction channels. *Semin. Cell Biol.* **3**, 3-16.

Laird, D. W. (2006). Life cycle of connexins in health and disease. *Biochem. J.* **394**, 527-543.

Lampe, P. D., Cooper, C. D., King, T. J. and Burt, J. M. (2006). Analysis of Connexin43 phosphorylated at S325, S328 and S330 in normoxic and ischemic heart. *J. Cell Sci.* **119**, 3435-3442.

Larsen, W. J. (1977). Structural diversity of gap junctions. A review. *Tissue Cell* **9**, 373-394.

Larsen, W. J., Wert, S. E. and Brunner, G. D. (1987). Differential modulation of rat follicle cell gap junction populations at ovulation. *Dev. Biol.* **122**, 61-71.
Merk, F. B., Albright, J. T. and Botticelli, C. R. (1973). The fine structure of granulosa cell nexuses in rat ovarian follicles. *Anat. Rec.* **175**, 107-125.
Micheva, K. D. and Smith, S. J. (2007). Array tomography: a new tool for imaging the molecular architecture and ultrastructure of neural circuits. *Neuron* **55**, 25-36.
Mühlfeld, C. and Richter, J. (2006). High-pressure freezing and freeze substitution of rat myocardium for immunogold labeling of connexin 43. *Anat. Rec. A. Discov. Mol. Cell. Evol. Biol.* **288A**, 1059-1067.
Nimlamool, W., Andrews, R. M. K. and Falk, M. M. (2015). Connexin43 phosphorylation by PKC and MAPK signals VEGF-mediated gap junction internalization. *Mol. Biol. Cell* **26**, 2755-2768.
Norris, R. P., Freudzon, M., Mehlmann, L. M., Cowan, A. E., Simon, A. M., Paul, D. L., Lampe, P. D. and Jaffe, L. A. (2008). Luteinizing hormone causes MAP kinase-dependent phosphorylation and closure of connexin 43 gap junctions in mouse ovarian follicles: one of two paths to meiotic resumption. *Development* **135**, 3229-3238.
Okuma, A., Kuraoka, A., Iida, H., Inai, T., Wasano, K. and Shibata, Y. (1996). Colocalization of connexin 43 and connexin 45 but absence of connexin 40 in granulosa cell gap junctions of rat ovary. *J. Reprod. Fertil.* **107**, 255-264.
Piehl, M., Lehmann, C., Gumpert, A., Denizot, J.-P., Segretain, D. and Falk, M. M. (2007). Internalization of large double-membrane intercellular vesicles by a clathrin-dependent endocytic process. *Mol. Biol. Cell* **18**, 337-347.
Rubio, M. E. and Wenthold, R. J. (1997). Glutamate receptors are selectively targeted to postsynaptic sites in neurons. *Neuron* **18**, 939-950.
Sirnes, S., Kjenseth, A., Leithe, E. and Rivedal, E. (2009). Interplay between PKC and the MAP kinase pathway in Connexin43 phosphorylation and inhibition of gap junction intercellular communication. *Biochem. Biophys. Res. Commun.* **382**, 41-45.
Smyth, J. W., Zhang, S.-S., Sanchez, J. M., Lamouille, S., Vogan, J. M., Hesketh, G. G., Hong, T. T., Tomaselli, G. F. and Shaw, R. M. (2014). A 14-3-3 mode-1 binding motif initiates gap junction internalization during acute cardiac ischemia. *Traffic* **15**, 684-699.
Solan, J. L. and Lampe, P. D. (2016). Kinase programs spatiotemporally regulate gap junction assembly and disassembly: effects on wound repair. *Semin. Cell Dev. Biol.* **50**, 40-48.
Terasaki, M., Shemesh, T., Kasthuri, N., Klemm, R. W., Schalek, R., Hayworth, K. J., Hand, A. R., Yankova, M., Huber, G., Lichtman, J. W. et al. (2013). Stacked endoplasmic reticulum sheets are connected by helicoidal membrane motifs. *Cell* **154**, 285-296.
Walton, J. (1979). Lead asparate, an en bloc contrast stain particularly useful for ultrastructural enzymology. *J. Histochem. Cytochem.* **27**, 1337-1342.
Watanabe, H., Washioka, H. and Tonosaki, A. (1988). Gap junction and its cytoskeletal undercoats as involved in invagination-endocytosis. *Tohoku J. Exp. Med.* **156**, 175-190.
White, T. W. and Paul, D. L. (1999). Genetic diseases and gene knockouts reveal diverse connexin functions. *Annu. Rev. Physiol.* **61**, 283-310.

Supplemental Information

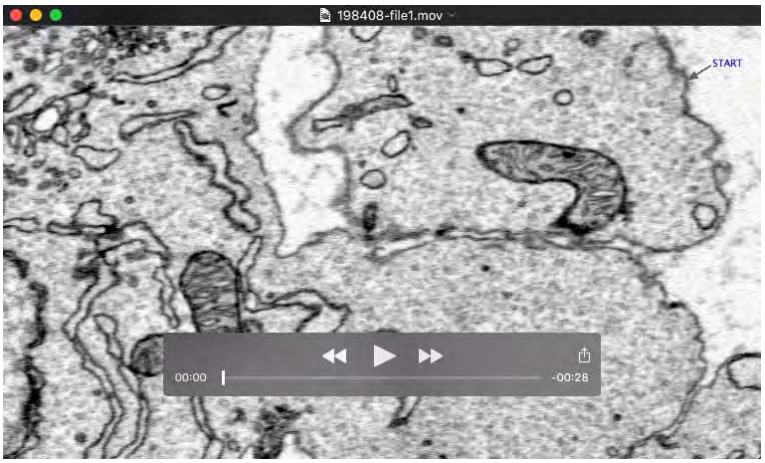

Movie 1. A thin cell process forming an invaginated gap junction with another granulosa cell. Serial z-plane sections of the same structure as Fig. 2B with more sections and a larger field of view.

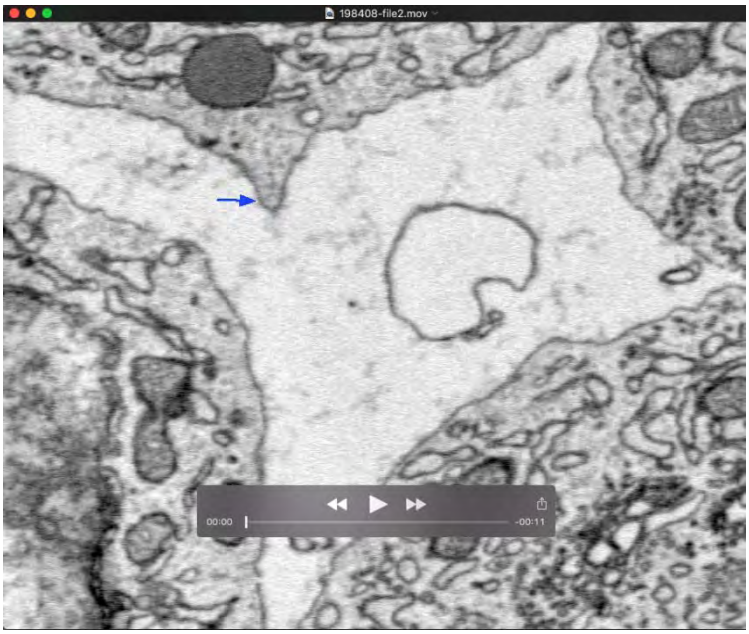

Movie 2. A second example of a cell process forming an invaginated gap junction with another granulosa cell.

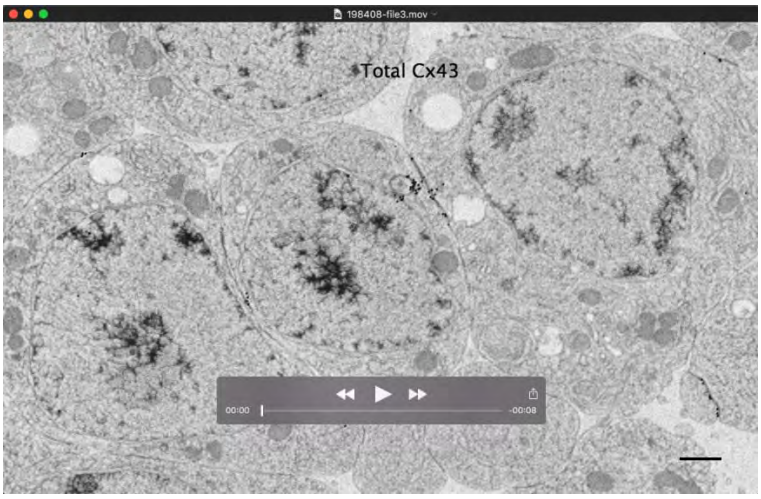

Movie 3. Immunogold labeling of total Cx43 in granulosa cells. A lower magnification view of Fig. 3A. Several gap junctions and connexosomes are visible and labeled with total Cx43. There is very little labeling of other structures. Scale bar is 1 micrometer.

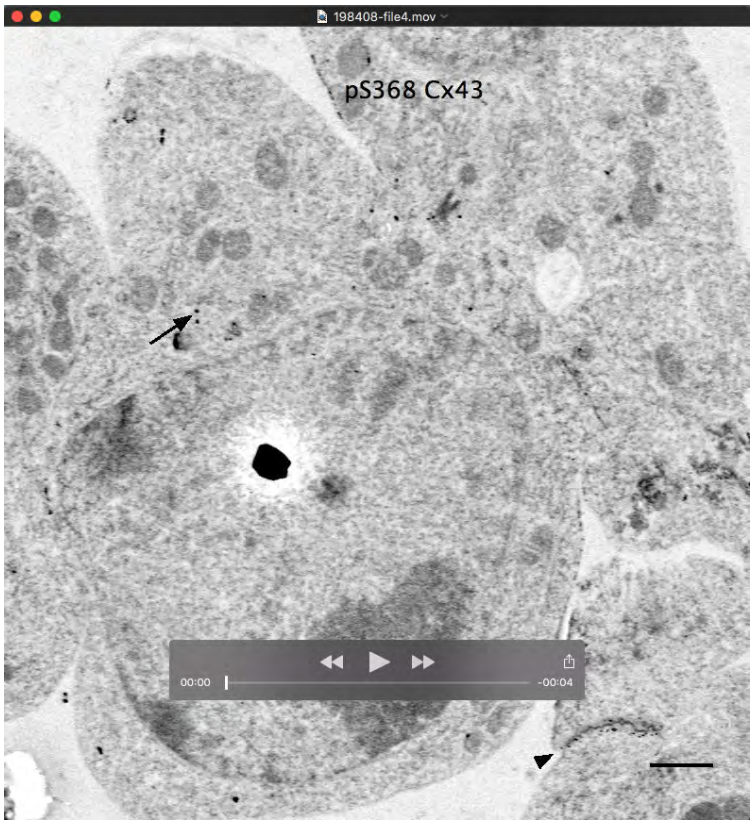

Movie 4. Immunogold labeling of pS368 Cx43 in granulosa cells. A lower magnification view of Fig. 4A. An arrow labels three connexosomes, and an arrowhead labels a gap junction near a connexosome. There is very little labeling of other structures. Scale bar is 1 micrometer.

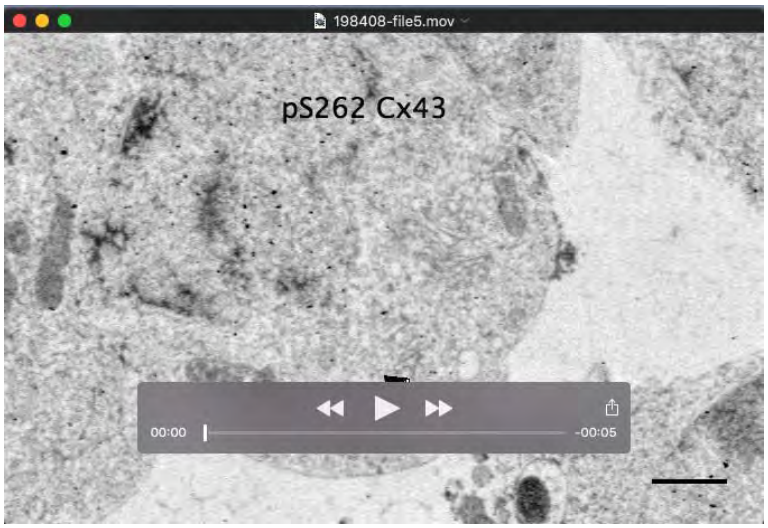

Movie 5. Immunogold labeling of pS262 and total Cx43 in granulosa cells. A lower magnification view of Fig. 7A, top row. The arrow labels a connexosome that is positive for both pS262 and total Cx43. There is some non-specific labeling of the nucleus. Scale bar is 1 micrometer.